

Structure of forecast error covariance in coupled atmosphere-chemistry data assimilation

Seon Ki Park^{1,2,3,4}, Sujeong Lim^{2,3}, and Milija Zupanski⁵

¹Department of Environmental Science and Engineering, Ewha Womans University, Seoul, Republic of Korea

²Department of Atmospheric Science and Engineering, Ewha Womans University, Seoul, Republic of Korea

³Center for Climate/Environment Change Prediction Research, Ewha Womans University, Seoul, Republic of Korea

⁴Severe Storm Research Center, Ewha Womans University, Seoul, Republic of Korea

⁵Cooperative Institute for Research in the Atmosphere, Colorado State University, Fort Collins, Colorado, USA

Correspondence to: Seon Ki Park (spark@ewha.ac.kr)

Abstract. In this study, we examined the structure of an ensemble-based coupled atmosphere-chemistry forecast error covariance. The Weather Research and Forecasting (WRF) model coupled with Chemistry (WRF-Chem), a coupled atmosphere-chemistry model, was used to create an ensemble error covariance. The control variable includes both the dynamical and chemistry model variables. A synthetic single observation experiment was designed in order to evaluate the cross-variable components of a coupled error covariance. The results indicate that the coupled error covariance has important cross-variable components that allow a physically meaningful adjustment of all control variables. The additional benefit of the coupled error covariance is that a cross-component impact is allowed, e.g., atmospheric observations can exert impact on chemistry analysis, and vice versa. Given the realistic structure of ensemble forecast error covariance produced by the WRF-Chem, we anticipate the ensemble-based coupled atmosphere-chemistry data assimilation will respond similarly to assimilation of real observations.

1 Introduction

The regional air quality is affected by synoptic weather situations or air masses with special chemical properties (Grell et al., 2000). In prediction of air quality, the coupled physical and chemical processes are essential, which include transport, deposition, emission, chemical transformation, aerosol interactions, photolysis, and radiation (Grell et al., 2005). Optimized initial conditions for a numerical model, including such coupled processes, can be obtained by data assimilation (DA; e.g., Houtekamer and Mitchell, 1998; Eibern and Schmidt, 1999; Wang et al., 2001; Evensen, 2003;

20 Park and Zupanski, 2003; Navon, 2009; Zupanski, 2009). Therefore, DA for an air quality prediction system could be approached as a coupled atmosphere-chemistry DA, with interaction between atmospheric and chemistry components. In typical data assimilation methodologies, such as variational and ensemble, the interaction between different variables is achieved by forecast error covariance, in particular its cross-variable components. Therefore, it is of fundamental interest for the development
25 of atmosphere-chemistry DA to investigate the coupled forecast error covariance. Here, we investigate the structure of the atmosphere-chemistry forecast error covariance using ensemble forecasting, which corresponds to the prediction step of an ensemble data assimilation algorithm (e.g., Zupanski, 2005, 2009).

2 Methodology and Synoptic Case

30 In this research, we use the Weather Research and Forecasting (WRF) model coupled with Chemistry (WRF-Chem) as a prediction model (Grell et al., 2005). The chosen chemistry option is the Carbon-Bond Mechanism version Z (CBMZ), which simulates the emission, transport, mixing, and chemical transformation of trace gases and aerosols simultaneously with meteorology and investigates the regional-scale air quality. More details on the WRF-Chem and corresponding options used in this
35 study are described in Appendix A.

We chose a synoptic case on 03 September 2005 related to Typhoon Nabi (2005), characterized by an increased impact on the Korean Peninsula. The experiment begins at 0000 UTC and ends at 0600 UTC on 03 September 2005. The WRF-Chem is set up with a horizontal resolution of 30 km and 28 vertical levels. Model domain is centered over the Korean Peninsula, covering an area of
40 approximately 3900 km x 4400 km with 132 x 147 horizontal grid points.

The ensemble forecast includes 32 ensemble members with a 6-hour assimilation window. The lateral boundary conditions are provided by the National Center for Environmental Prediction (NCEP) Global Forecasting System (GFS). The control variables defined in DA (i.e., variables adjusted during DA) are the WRF-Chem prognostic variables that include dynamical variables such as winds,
45 perturbation potential temperature, perturbation geopotential, water vapor mixing ratio and perturbation dry air mass in column, and the chemical variables such as ozone (O_3), nitrates (NO, NO_2 , NO_3) and sulfur dioxide (SO_2) as well.

3 Experimental Design

A common approach to investigating forecast error covariance in data assimilation is to conduct a
50 single observation experiment (Thepaut et al., 1996; Whitaker et al., 2009; Buehner et al., 2010), in which only one observation is assimilated using the full DA system. The analysis increments (i.e., analysis minus guess) from such an experiment show how the observation information is distributed spatially and among different analysis variables (e.g., Buehner, 2005). However, in order to

investigate the structure of a coupled forecast error covariance before real observations are available
 55 and even before the full DA algorithm is developed, one can consider the assimilation of a single
 synthetic observation located at a chosen model grid point. In particular, we define the synthetic
 observation as

$$y_{synth} = x^f + \sigma_o \quad (1)$$

where x^f is the forecast and σ_o is the observation error standard deviation. Following *Thepaut et al.*
 [1996, Eq. (3)], with some modifications and using (1), the analysis increment in a single synthetic
 60 observation experiment is

$$x^a - x^f = \mathbf{P}_f \left(\frac{\sigma_o}{\sigma_f^2 + \sigma_o^2} \right)_{ijk} \quad (2)$$

where x^a is the analysis, σ_f is the forecast error standard deviation, and the subscript ijk defines
 the grid location of the pseudo-observation point. Equation (2) indicates that analysis increment
 represents the ijk -th column of the forecast error covariance scaled by standard deviations of obser-
 vation error and forecast error. In our experiments the forecast error covariance is ensemble-based,
 65 as defined in Zupanski (2005) as:

$$\mathbf{P}_f = \mathbf{P}_f^{1/2} (\mathbf{P}_f^{1/2})^T, \quad \mathbf{P}_f^{1/2} = \begin{pmatrix} p_1^f & \cdots & p_N^f \end{pmatrix}, \quad p_n^f = m(x_0^n) - m(x_0) \quad (3)$$

where the superscript T denotes the transpose, the index n refers to ensemble member, N is the total
 number of ensemble forecasts, m represents the nonlinear WRF-Chem model, and the subscript 0
 denotes the initial time of the forecast with corresponding initial conditions x_0 and ensemble initial
 conditions x_0^n . In this experiment, the control initial conditions are obtained by interpolation from
 70 the NCEP GFS model, while the initial ensemble perturbations are created using the lagged forecast
 outputs.

Since we are interested in the coupled atmosphere-chemistry forecast error covariance, we design
 two experiments with: (i) synthetic temperature observation at 250 hPa located at a grid point near
 (132E, 23N), on the northwest side of the typhoon, and (ii) synthetic ozone observation at 250 hPa
 75 located at a grid point near the eye of the typhoon (134E, 21N).

4 Results

We show the impact of single synthetic temperature (T) and ozone (O_3) observations in terms of the
 analysis increments $x^a - x^f$ impacting all control variables. As mentioned earlier, our main interest
 is to examine the cross-variable covariance structure between atmospheric and chemistry variables,
 80 since the cross-variable analysis impact is possible only because of the multivariate structure of the
 coupled ensemble forecast error covariance.

In Fig. 1 we show the impact of synthetic T observation at 250 hPa on the analysis increments of
 T, O_3 , nitrogen-dioxide (NO_2), and sulfur dioxide (SO_2). The analysis increment of T at 250 hPa

(e.g., at the same level of synthetic T observation) shows a typical response with nearly circular
85 isolines with the maximum of 0.4 K at the observation location (Fig. 1a). The analysis increments of
O₃, NO₂, and SO₂ are also shown in vertical cross-sections. One can see that O₃ (Fig. 1b) and NO₂
(Fig. 1c) analyses have the largest change at the level of single T observation, while the SO₂ analysis
(Fig. 1d) is mostly impacted near 700 hPa (approximately σ -level 13). This is likely a consequence
90 of the vertical structure of O₃ and NO₂ with the largest values in the upper troposphere and the
stratosphere, while SO₂ has typically the largest values in the lower troposphere (e.g., Meena et al.,
2006). The strongest impact of T observation is on O₃, with the magnitude up to 0.001 ppmv, while
the magnitude is somewhat smaller for NO₂ and SO₂. One can also infer that an increase of T will
imply a decrease of O₃, NO₂, and SO₂. Probably the most important implication of these results is
95 that observations of an atmospheric variable (e.g., temperature) can change the analysis of chemical
variables in a physically meaningful way. This means that even with no chemistry observations in
the local area, the analysis of chemical variables can still be adjusted in agreement with standard
dynamical variables of the model. On the other hand, if there are chemistry observations in the
area, the chemistry analysis change introduced by atmospheric observations will act as an additional
dynamical constraint to the final analysis.

100 In Fig. 2 the impact of O₃ single observation at 250 hPa on itself and the other variables is shown.
As before, we focus on the vertical cross-section of the analysis response. The impact of O₃ obser-
vation on its own analysis shows the anticipated response with the largest magnitude at observa-
tion location, approximately 0.02 ppmv (Fig. 2a). Although smaller in magnitude, the analysis incre-
ments of NO₂ (Fig. 2b) and SO₂ (Fig. 2c) show the vertical structure with maxima in the upper and
105 lower troposphere, respectively. It is also notable that an increase of O₃ brings about an increase of
NO₂ and SO₂, confirming the direct relationship between these variables as noticed in Fig. 1. The
T analysis increment indicates that there is a cooling at the level of O₃ observation, while there is a
warming above and below (Fig. 2d).

The results shown in Figs. 1 and 2 indirectly confirm that the improved stratospheric ozone dis-
110 tribution by DA can make a better representation of stratospheric winds, temperature and other con-
stituents (e.g., Lahoz et al., 2007).

5 Conclusions

The structure of an ensemble-based coupled atmosphere-chemistry forecast error covariance was
examined in the context of the WRF-Chem model. A synthetic single observation experiment was
115 designed in order to evaluate the cross-variable components of the coupled error covariance. Our re-
sults indicate that the coupled error covariance has important cross-variable components that allow
a physically meaningful adjustment of all control variables, and a much wider impact of observa-
tions (e.g., atmospheric observation on chemistry analysis, and vice versa). The analysis increments

created in response to synthetic temperature and ozone observations illustrate the complexity of
120 atmosphere-chemistry cross-correlations and the forecast error covariance structure. Given the realistic structure of ensemble forecast error covariance produced by the WRF-Chem, we anticipate the ensemble-based coupled atmosphere-chemistry data assimilation will respond similarly to assimilation of real observations. Therefore, our next step is to apply the WRF-Chem with an ensemble-based data assimilation algorithm (e.g., the maximum likelihood ensemble filter (MLEF); Zupanski, 2005)
125 to assimilation of real chemical and atmospheric observations.

Appendix A: Description on the WRF-Chem

In this research, we use the Weather Research and Forecasting (WRF) model coupled with Chemistry (WRF-Chem) version 3.4.1 as a prediction model in a regional-scale. As a coupled model, it simulates the emission, transport, mixing and chemical transformation of trace gases and aerosols
130 simultaneously with meteorology using the governing equations with mass and scalar conserving flux form and the terrain-following mass vertical coordinate system (Grell et al., 2005; Fast et al., 2006). Therefore, it uses the same transport scheme, horizontal and vertical coordinates, and physics schemes with the same time step (Grell et al., 2005; Fast et al., 2006). Figure A1 represents the flow chart of the WRF-Chem model. It is made up of the WRF Pre-processing System (WPS), the
135 WRF-Chem model, and the visualization processes. The WPS creates the meteorology data with the terrestrial data and the meteorology initial conditions (ICs) and boundary conditions (BCs) which are provided by the National Center for Environmental Prediction (NCEP) Global Forecasting System (GFS) producing the global latitude/longitude 1 degree resolution and terrestrial data. In the WRF-Chem model, the chemical ICs and BCs are automatically obtained by the climatology. Fur-
140 thermore, it simulates the evolution of chemical species with the prognostic variables that include both dynamical and chemical variables. For the ensemble experiments, the initial ensemble perturbations are created using the 12-hour lagged forecast outputs. Finally, the Advanced Research WRF post-processing (ARWpost) along with Grid Analysis and Display System (GrADS) is used for the visualization process.

145 We also discuss various physical and chemical processes employed in the WRF-Chem model in more detail. Table A1 summarizes the WRF-Chem configuration options what are used in this study. To evaluate the cross-variable component of forecast error covariance, we select the simplified dynamics rather than sophisticated physical processes. Regarding the atmospheric processes, we use the recommended physics options for the regional climate case at 30 km grid size in our experiments.
150 As the chemical options, the Carbon Bond Mechanism version Z (CBM-Z) without Dimethylsulfide scheme is used for the gas-phase chemistry. The CBM-Z photochemical mechanism contains 55 prognostic species and 134 reactions having the lumped structure approach for condensing organic chemical species and reactions (Fast et al., 2006). It also uses a regime dependent approach based

on the partitioned kinetics, such as background, anthropogenic, and biogenic submechanisms for
155 saving the computational time (Fast et al., 2006). Furthermore, we consider the chemical tendency
diagnostic for equation budget analysis. However, we did not consider the convective parameteri-
zation which can simulate the subgrid convective transport, wet scavenging, and aqueous chemistry
due to simple experiment setting, even with a typhoon case.

Acknowledgements. This work is supported by the Korea Environmental Industry & Technology Institute
160 through the Eco Innovation Program (ARQ201204015), and partly by the National Research Foundation of
Korea grant (No. 2009-0083527) funded by the Korean government (MSIP). The third acknowledges a partial
support from the National Science Foundation Collaboration in Mathematical Geosciences Grant 0930265 and
from the NASA Modeling, Analysis and Prediction (MAP) Program Grant NNX10AG92G.

References

- 165 Buehner, M.: Ensemble-derived stationary and flow-dependent background-error covariances, *Q. J. R. Meteorol. Soc.*, 131, 1013–1043, 2005.
- Buehner, M., Houtekamer, P. L., Charette, C., Mitchell, H. L., and He, B.: Intercomparison of variational data assimilation and the ensemble kalman filter for global deterministic NWP. Part I: Description and single-observation experiments, *Mon. Wea. Rev.*, 138, 1567–1586, 2010.
- 170 Eibern, H., and Schmidt, H.: A four-dimensional variational chemistry data assimilation scheme for Eulerian chemistry transport modeling, *J. Geophys. Res.*, 104(D15), 18583–18598, 1999.
- Evensen, G.: The ensemble Kalman filter: theoretical formulation and practical implementation, *Ocean Dyn.*, 53, 343–367, 2003.
- Fast, J. D., Gustafson Jr., W. I., Easter R. C., Zaveri R. A., Barnard J. C., Chapman E. G., Grell G. A.,
175 and Peckham S. E.: Evolution of ozone, particulates, and aerosol direct radiative forcing in the vicinity of Houston using a fully coupled meteorology-chemistry-aerosol model, *J. Geophys. Res.*, 111, D21305, doi:10.1029/2005JD006721, 2006.
- Grell, G. A., Emeis, S., Stockwell, W. R., Schoenemeyer, T., Forkel, R., Michalakes, J., Knoche, R., and Seidl, W.: Application of a multiscale, coupled MM5/chemistry model to the complex terrain of the VTALP valley
180 campaign, *Atmos. Environ.*, 34, 1435–1453, 2000.
- Grell, G. A., Peckham, S. E., Schmitz, R., McKeen, S. A., Frost, G., Skamarock, W. C., and Eder, B.: Fully coupled “online” chemistry within the WRF model, *Atmos. Environ.*, 39, 6957–6975, 2005.
- Houtekamer, P. L., and Mitchell, H. L.: Data assimilation using an ensemble Kalman filter technique, *Mon. Wea. Rev.*, 126, 796–811, 1998.
- 185 Lahoz, W. A., Errera, Q., Swinbank, R., and Fonteyn, D.: Data assimilation of stratospheric constituents: a review, *Atmos. Chem. Phys.*, 7, 5745–5773, 2007.
- Meena, G. S., Bhosale, C. S., and Jadhav, D. B.: Retrieval of stratospheric O₃ and NO₂ vertical profiles using zenith scattered light observations, *J. Earth Syst. Sci.*, 115(3), 333–347, 2006.
- Navon, I. M.: Data assimilation for numerical weather prediction: A review, in: *Data Assimilation for Atmospheric, Oceanic and Hydrologic Applications*, Park, S. K. and Xu, L., Eds., Springer, Berlin-Heidelberg,
190 21–65, 2009.
- Park, S. K., and Zupanski, D.: Four-dimensional variational data assimilation for mesoscale and storm-scale applications, *Meteorol. Atmos. Phys.*, 82, 173–208, 2003.
- Thepaut, J.-N., Courtier, P., Belaud, G., and Lemaitre, G.: Dynamical structure functions in a four-dimensional
195 variational assimilation: A case study, *Q. J. R. Meteorol. Soc.*, 122, 535–561, 1996.
- Wang, K.-Y., Lary, D. J., Shallcross, D. E., Hall, S. M., and Pyle, J. A.: A review on the use of the adjoint method in four-dimensional atmospheric-chemistry data assimilation, *Q. J. R. Meteorol. Soc.*, 127, 2181–2204, 2001.
- Whitaker, J. S., Compo, G. P., and Thepaut, J.-N.: A comparison of variational and ensemble-based data assimilation systems for reanalysis of sparse observations, *Mon. Wea. Rev.*, 137, 1991–1999, 2009.
- 200 Zupanski, M.: Maximum likelihood ensemble filter: Theoretical aspects, *Mon. Wea. Rev.*, 133, 1710–1726, 2005.
- Zupanski, M.: Theoretical and practical issues of ensemble data assimilation in weather and climate, in: *Data Assimilation for Atmospheric, Oceanic and Hydrologic Applications*, Park, S. K. and Xu, L., Eds., Springer,

Berlin-Heidelberg, 67–84, 2009.

205

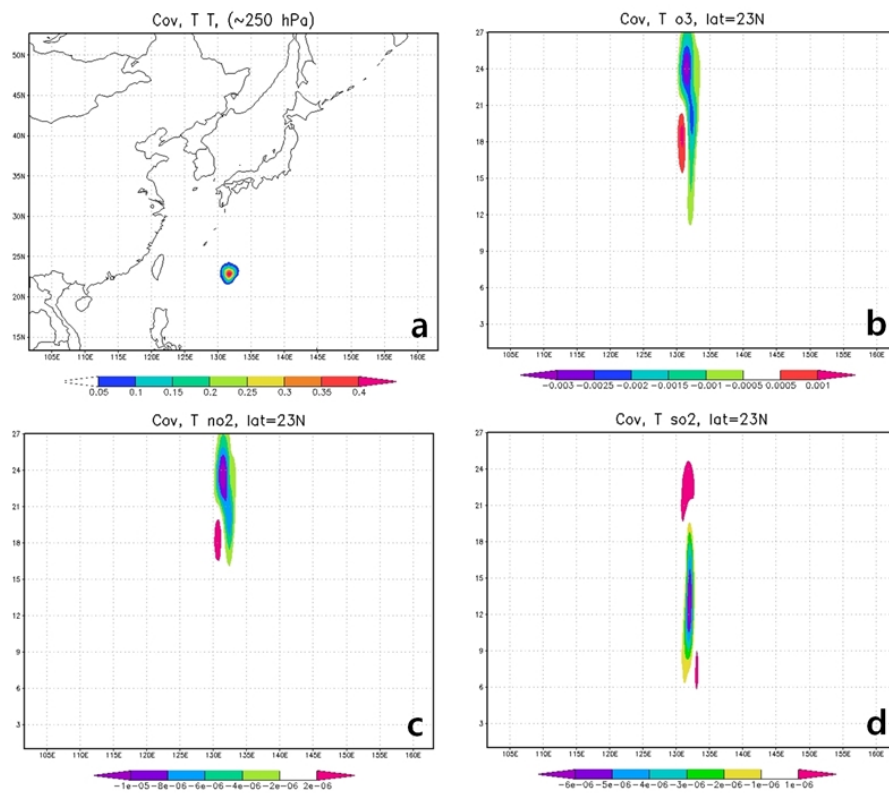


Figure 1. The analysis increments ($x^a - x^f$) in response to a single T observation at 250 hPa (near σ -level 24): (a) horizontal response of T at 250 hPa, and vertical responses of (b) O₃, (c) NO₂ and (d) SO₂. In (b)-(d), the vertical axis represents the vertical σ -levels. Units are ppmv for chemical variables and K for temperature.

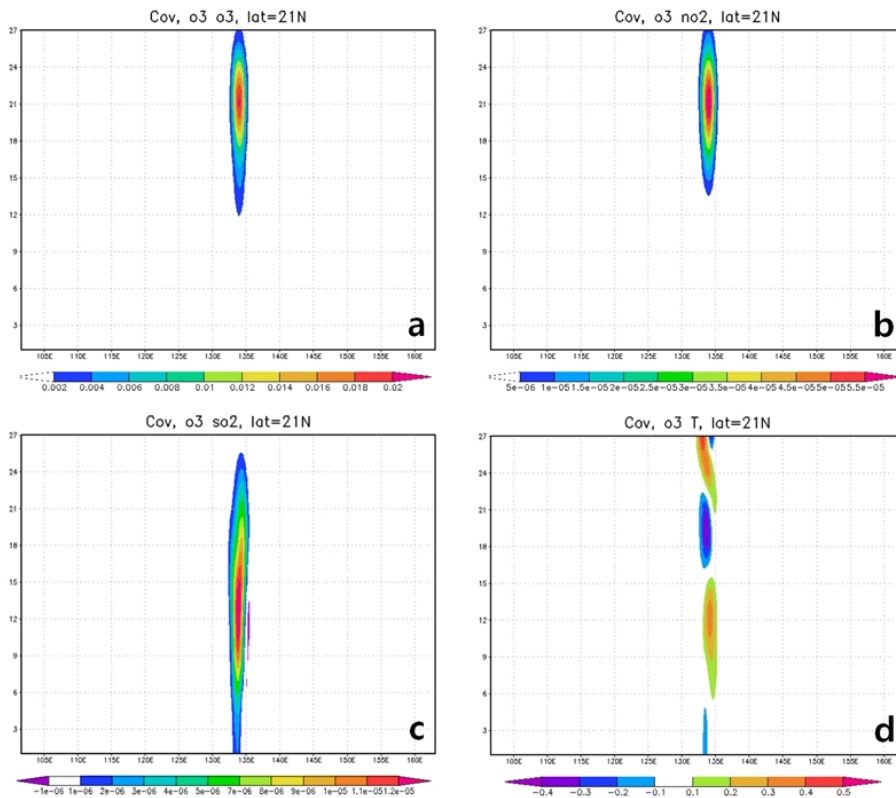


Figure 2. Same as in Fig. 1 but for vertical cross-section of the analysis increments ($x^a - x^f$) in response to a single O₃ observation at 250 hPa for (a) O₃, (b) NO₂, (c) SO₂ and (d) T.

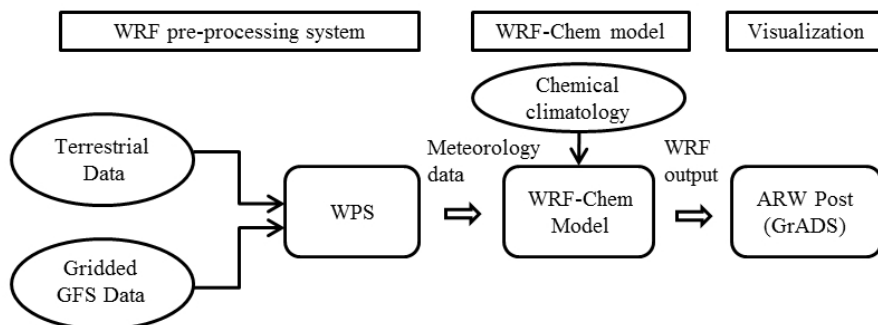


Figure A1. Flowchart of the WRF-Chem model.

Table A1. Selected WRF-Chem configuration options.

Atmospheric Process	WRF-Chem Option
Microphysics	WSM 6-class graupel
Longwave radiation	CAM
Shortwave radiation	CAM
Surface layer	Revised MM5 Monin-Obukhov
Land surface	Unified Noah LSM
Planetary boundary layer	YSU
Cumulus parameterization	Kain-Fritsch (new Eta)
Gas-phase chemistry	CBM-Z